Analytical Biochemistry 669 (2023) 115118

Contents lists available at ScienceDirect

Analytical Biochemistry

journal homepage: www.elsevier.com/locate/yabio

Selection of G-rich ssDNA aptamers for the detection of enterotoxins of the cholera toxin family

Nerissa A. Molejon [a], Catherine M. Lapada [a], Vasso Skouridou [b,**], Analiza P. Rollon [a], Mohammed S. El-Shahawi [c], Abdulaziz S. Bashammakh [c], Ciara K. O'Sullivan [b,d,*]

[a] Environmental Engineering Program, National Graduate School of Engineering, University of the Philippines, Diliman, 1101, Quezon City, Philippines
[b] Interfibio Research Group, Departament d'Enginyeria Química, Universitat Rovira i Virgili, Avinguda Països Catalans 26, 43007, Tarragona, Spain
[c] Department of Chemistry, Faculty of Science, King Abdulaziz University, Jeddah, Kingdom of Saudi Arabia
[d] Institució Catalana de Recerca i Estudis Avançats (ICREA), Passeig Lluís Companys 23, 08010, Barcelona, Spain

ARTICLE INFO

Keywords:
Vibrio cholerae
Enterotoxigenic *Escherichia coli*
AB_5 enterotoxins
DNA aptamer
Next generation sequencing
G-rich sequence motif

ABSTRACT

Cholera and milder diarrheal disease are caused by *Vibrio cholerae* and enterotoxigenic *Escherichia coli* and are still a prominent public health concern. Evaluation of suspicious isolates is essential for the rapid containment of acute diarrhea outbreaks or prevention of epidemic cholera. Existing detection techniques require expensive equipment, trained personnel and are time-consuming. Antibody-based methods are also available, but cost and stability issues can limit their applications for point-of-care testing. This study focused on the selection of single stranded DNA aptamers as simpler, more stable and more cost-effective alternatives to antibodies for the co-detection of AB_5 toxins secreted by enterobacteria causing acute diarrheal infections. Cholera toxin and *Escherichia coli* heat-labile enterotoxin, the key toxigenicity biomarkers of these bacteria, were immobilized on magnetic beads and were used in a SELEX-based selection strategy. This led to the enrichment of sequences with a high % GC content and a dominant G-rich motif as revealed by Next Generation Sequencing. Enriched sequences were confirmed to fold into G-quadruplex structures and the binding of one of the most abundant candidates to the two enterotoxins was confirmed. Ongoing work is focused on the development of monitoring tools for potential environmental surveillance of epidemic cholera and milder diarrheal disease.

1. Introduction

Diarrheal disease is a leading cause of morbidity and mortality in developing countries and especially among young children [1]. It is transmitted through the consumption of contaminated food and water [2] and it affect millions of people globally [3]. The enteric bacteria species responsible for this disease include *Salmonella* spp., *Campylobacter* spp., enterotoxigenic and enteropathogenic *Escherichia coli*, *Shigella* spp. and *Vibrio cholerae* [4]. Two of the most common bacterial species causing diarrhea particularly in low- and middle-income countries are *Vibrio cholerae* and enterotoxigenic *Escherichia coli* (ETEC) [5,6].

V. cholerae thrives in saline waters as well as in warm, organic nutrient-rich freshwaters [7] and causes cholera, an acute diarrheal disease [8]. There are up to 4 million cases of cholera every year, with 143,000 deaths [9] and the disease is endemic in 69 countries, mainly affecting Africa and Asia [10]. Enterotoxigenic *E. coli* (ETEC) is typically found in drinking and environmental water in endemic areas in Asia, Africa and Latin America [11]. It is the main bacterial cause of travelers' diarrhea acquired by international travelers in low-income countries and of diarrhea in young children, with an estimated 840 million cases and more than 3.8 million deaths every year [12]. Both bacteria are transmitted through the fecal-oral route and once inside the host, they colonize the epithelium of the small intestine and secrete enterotoxins: *V. cholerae* produces the cholera toxin (CT) while ETEC produces the heat-labile (LT) and the heat-stable (ST) enterotoxins. ETEC strains can produce distinct variants of the toxins but the main one produced in humans is LT-I (referred to as LT-ETEC from here on), which is homologous to CT (82% sequence identity) [5]. Both CT and LT-ETEC belong to the AB_5 bacterial toxin family which also includes toxins produced by

* Corresponding author. Interfibio Research Group, Departament d'Enginyeria Química, Universitat Rovira i Virgili, Avinguda Països Catalans 26, 43007, Tarragona, Spain.
** Corresponding author.
E-mail addresses: vasoula.skouridou@urv.cat (V. Skouridou), ciara.osullivan@urv.cat (C.K. O'Sullivan).

https://doi.org/10.1016/j.ab.2023.115118
Received 15 January 2023; Received in revised form 11 March 2023; Accepted 14 March 2023
Available online 22 March 2023

Bordetella pertussis (pertussis toxin), *Shigella dysenteriae* (Shiga toxin) and Shiga-toxin producing *E. coli* (STEC) [13]. Toxins of this family are multimeric proteins composed of an A subunit heterodimer and a ring-shaped B subunit pentamer, forming an AB_5 complex of around 85 kDa [14]. The B subunits bind specific receptors on the host cells and enable the internalization of the catalytic A subunits which cause cellular toxicity by the efflux of ions and water from the host cells [13]. This can lead to severe dehydration and sometimes death within hours if proper treatment is not administered immediately. Illness caused by LT-ETEC though is less severe compared to CT [5].

Not all *V. cholerae* and ETEC strains produce enterotoxins, therefore it is important to determine the toxigenicity of isolates when assessing public health significance. Epidemic cholera is exclusively associated with toxigenic strains of the O1 and O139 serogroup [15] and testing isolates for CT production is essential in the early stages of an outbreak or when the incidence of cholera is low in endemic settings [16]. Besides diarrheal stool isolates, the US Centers for Disease Control and Prevention recommends that all food or environmental *V. cholerae* O1 isolates should also be tested for cholera toxin production after identification has been confirmed [9]. The clinical manifestations of ETEC are not as severe as those observed for cholera and as a result, LT-ETEC is not routinely detected in clinical microbiological laboratories in developed countries [6]. However, repeated infections by ETEC can promote enteropathies, malnutrition, reduce immune function and increase the use of antibiotics resulting in the spread of antimicrobial resistant bacteria [17]. Vaccines are currently under development in an effort to contain the consequences of ETEC infections. It is thus evident that detection of diarrhea-causing enterotoxins of the CT family (CT and LT-ETEC) is highly relevant for diagnostic purposes and patient management, as well as for prevention and control.

Cholera diagnostics are mainly based on microbiological and molecular methods [16], with the gold standard being conventional culture. However, the process is lengthy, requires laboratory infrastructure and skilled personnel and does not allow the detection of CT. Several methods do however exist for the detection of bacterial toxins [18]. Detection of CT and LT-ETEC enterotoxins is achieved by culturing suspicious isolates in growth media specifically formulated to induce *in vitro* toxin secretion [9,19]. More sensitive, rapid and specific identification of toxigenic strains of both *V. cholerae* and ETEC became possible with the implementation of molecular diagnostics targeting the major virulence factors of these bacteria, either employing thermal cycling [20–22] or isothermal [23–25] amplification. However, these approaches are generally laboratory-based requiring infrastructure and trained personnel. Similarly, antibody or nucleic acid-based bioanalytical assays offer sensitivity and specificity but are not suited to field testing [16,26–29]. Rapid diagnostic tests (RDTs) relying on enterotoxin-specific antibodies are promising tools for accurate and timely diagnosis and they can be easily performed at the point-of-care (POC) by non-specialized personnel [30,31]. In the case of cholera, the use of RDTs in low-resource settings is recommended by WHO's Global Task Force on Cholera Control [32] but they exhibit moderate sensitivity and specificity [33]. Moreover, high production costs, batch-to-batch variability observed with polyclonal antibodies, irreversible thermal denaturation and limited shelf life should also be considered when developing antibody-based assays for enterotoxin detection.

Aptamers offer an interesting cost-effective alternative to antibodies for the development of detection platforms, especially for POC applications. These synthetic DNA molecules can be selected against essentially any type of target via an iterative selection process termed SELEX [34,35]. Several properties of aptamers, such as high affinity and specificity, reproducible chemical synthesis, easy and low-cost modification, high stability and reversible denaturation have encouraged their use as biorecognition elements in diagnostics [36,37]. Their compatibility with POC diagnostics makes them particularly attractive for field deployment and on-site detection of pathogens [38,39].

Even though aptamers against a variety of bacterial toxins have been reported [40], there are only two reports detailing the selection of aptamers binding to enterotoxins of the AB_5 family, and both were against CT. The first report described a selection against the CT holotoxin and the enriched ssDNA pool after 5 rounds was shown to detect less than 40 ng of toxin by direct binding assays [41]. The second one targeted only the B subunit of CT and several high binding affinity aptamers were identified [42]. In this work we sought to develop aptamers against CT and LT-ETEC as potential biorecognition elements for the detection of diarrhea-causing enterobacteria *V. cholerae* and ETEC. The selection was performed using the two enterotoxins immobilized on magnetic beads in sequential incubation steps with the ssDNA library. Enriched oligonucleotide pools bound on each of the enterotoxin-magnetic beads from the last selection round were analyzed by Ion Torrent Next Generation Sequencing. Bioinformatic analysis revealed the presence of a highly enriched G-rich sequence motif in the majority of the sequences and led to the identification of a promising aptamer candidate confirmed to fold into a G-quadruplex for potential use in the diagnosis of *V. cholerae* and ETEC infections.

2. Materials and methods

2.1. Materials

Cholera toxin (CT) from *Vibrio cholerae* (ref. C8052), the polyclonal goat anti-cholera toxin B-subunit IgG antibody (ref. 227040), the polyclonal rabbit anti-goat IgG (whole molecule)-HRP conjugated IgG antibody (ref. A5420), N-hydroxysuccinimide (NHS), 4-morpholinoethanesulfonic acid (MES), skim milk powder, casein hydrolysate and yeast extract were purchased from Merck (Spain). Enterotoxigenic *Escherichia coli* double mutant heat-labile toxoid (dmLT) recombinant protein (LT-ETEC) was kindly provided by BEI Resources (ref. NR-51683). Dynabeads M-270 Amine magnetic beads, Dynabeads M-270 Epoxy magnetic beads, 1-ethyl-3-(3-dimethylaminopropyl) carbodiimide hydrochloride (EDC), sulfo–NHS–acetate, phosphate buffered saline (PBS; 10 mM phosphate, 137 mM NaCl, 2.7 mM KCl, pH 7.4), Tween-20, DreamTaq DNA polymerase, lambda exonuclease, T4 DNA ligase and GeneRuler Low Range DNA ladder were supplied by Fisher Scientific (Spain). The TMB Super Sensitive One Component HRP Microwell Substrate solution was from Surmodics (USA). The Zymo Research Oligo Clean & Concentrator kit and DNA Clean & Concentrator kits were supplied by Ecogen (Spain). The oligonucleotides were purchased from Biomers.net (Germany). All other reagents were from Fisher Scientific (Spain), Merck (Spain) and Scharlau (Spain). Milli-Q water was used for all experiments.

2.2. Preparation of enterotoxin-magnetic beads for SELEX

The immobilization of CT and LT-ETEC on amine-functionalized magnetic beads was achieved via EDC/NHS carbodiimide chemistry. In brief, 100 μL of Dynabeads M-270 Amine (30 mg/mL) were transferred to a 1.5 mL microtube and washed with 1 mL of 0.1 M MES pH 5 using magnetic separation. The beads were resuspended with 60 μL of 1 mg/mL CT or LT-ETEC in 0.1 M MES pH 5 or only MES for the control beads. Subsequently, 6 μL of a mixture containing 10 mg/mL EDC and 15 mg/mL NHS in 0.1 M MES pH 5 were added to each bead suspension, followed by incubation for 2 h at 22 °C under gentle tilt rotation. The supernatants were discarded, and the beads were resuspended with 100 μL of 1 mM sulfo–NHS–acetate in PBS to block any remaining unreacted amine groups. Following 1 h at 22 °C with slow tilt rotation, the beads were washed three times with 500 μL of PBS containing 0.05% (v/v) Tween-20 (PBST) and finally resuspended with 100 μL of PBS. The bead suspensions were stored at 4 °C until use. To verify the immobilization of the enterotoxins on the surface of the magnetic beads, a bead-based ELISA assay was performed. To this end, 2 μL of each bead suspension (CT-beads, LT-ETEC-beads, and control-beads) were transferred to a 1.5

mL microtube individually and 100 μL of 5% (w/v) skim dry milk in PBST were added for blocking (30 min at 22 °C under rotation). The beads were washed three times with 100 μL of PBST and then resuspended with 100 μL of goat anti-cholera toxin B-subunit IgG antibody (1/5000 dilution in 1% (w/v) milk in PBST) followed by a 30 min-incubation at 22 °C under rotation. The beads were then washed three times with 100 μL of PBST and then resuspended with 100 μL of polyclonal rabbit anti-goat IgG-HRP conjugated IgG antibody (1/20000 dilution in 1% (w/v) milk in PBST). They were incubated for 30 min at 22 °C under rotation, followed by washing with PBST (3 × 100 μL) and resuspending with 50 μL of TMB ELISA substrate. The color change from colorless (negative) to blue (positive) was monitored and the enzymatic reaction was stopped by adding 50 μL of 1 M H_2SO_4. The solutions were magnetically separated from the beads and transferred to the wells of a 96-well plate for measuring the absorbance at 450 nm using a microplate reader.

2.3. Aptamer selection process

The selection was performed for 20 rounds (Table 1) using PBS with 1.5 mM $MgCl_2$ as the selection buffer and magnetic beads with immobilized enterotoxins. The initial ssDNA library pool had a random region of 40 nt flanked by primer annealing sites of 18 nt each (5′-AAGCATCCGCTGGTTGAC-N40-ATGCCATTTGGGCTGCTC-3′, 76 nt). Before each selection round, the ssDNA (sub)pool was diluted in selection buffer and heated for 2 min at 95 °C followed by slow cooling to 22 °C. For the 1st round, 100 μL of 3 μM of the re-folded ssDNA library in selection buffer was incubated with 5 μL of CT-beads for 1 h. The beads were washed three times with 100 μL of binding buffer and resuspended in 20 μL of the same buffer. Negative selection with control-beads was performed in round 2, by first incubating the ssDNA prepared from round 1 with 2 μL of control-beads for 30 min. The unbound ssDNA pool was transferred to a tube with 2 μL of CT-beads followed by incubation for 30 min. Control-beads and CT-beads were washed (3 × 100 μL of binding buffer) and resuspended with 20 μL of binding buffer. Selection with the LT-ETEC was incorporated in round 10. In this case, the ssDNA pool was first incubated with the control-beads, the unbound fraction was incubated with LT-ETEC-beads, followed by incubation of the unbound fraction with the CT-beads. Two microliters of each bead suspension were used and all incubation steps were performed at 22 °C under tilt rotation. To prepare ssDNA for each selection round, ssDNA bound on the CT-beads was first amplified by PCR using 3 μL of bead suspension per 100 μL of PCR master mix containing 200 nM of each unmodified forward primer and 5′-phosphate-modified reverse primer. The PCR steps consisted of 2 min at 95 °C, followed by 5–20 cycles of 15 s at 95 °C, 15 s at 58 °C and 15 s at 72 °C. The PCR reactions served as the templates for asymmetric PCR, which was performed for 11–12 cycles using a master mix containing only forward primer (400 nM) and 1/10 volume of PCR reaction. Lambda exonuclease (15 U) was then added to the asymmetric PCR reaction to digest the double stranded DNA for 2 h at 37 °C, followed by enzyme deactivation at 80 °C for 10 min. Single stranded DNA was finally purified using the Oligo Clean & Concentrator kit. Pilot PCR was performed at the end of each selection round to determine the number of PCR cycles required for optimum amplification of CT-bound ssDNA. All steps were analyzed by agarose gel electrophoresis.

Table 1
Selection strategy for the identification of CT-binding ssDNA aptamers.

Round	Magnetic beads	Duration
1	CTX-beads	1 h
2–9	Control-beads → CTX-beads	30 min
10–20	Control-beads → LT-ETEC-beads → CTX-beads	30 min

2.4. Evolution study

To study the progress of the selection, ssDNA was initially prepared from several rounds (1, 2, 4, 6, 10, 12, 17) by PCR amplification of ssDNA bound to CT-beads from each of these rounds, followed by asymmetric PCR and lambda exonuclease digestion, as detailed earlier. Following purification and re-folding, 50 μL of 100 nM ssDNA from each round were incubated with 1 μL of CT-beads for 30 min at 22 °C under tilt rotation. Following incubation, the beads were washed three times with 100 μL of selection buffer and resuspended with 10 μL of the same buffer. Bead-bound ssDNA was detected after 10 cycles of PCR using the same conditions described above, followed by visualization of the amplicons using agarose gel electrophoresis. The intensities of the bands corresponding to the PCR amplicons were estimated using the ImageJ software and the gel analysis option.

2.5. Next Generation Sequencing (NGS)

The ssDNA pools bound on the CT-beads and the LT-ETEC-beads from the final selection round (round 20) as well as the CT-bound ssDNA pool from round 6 were chosen for analysis with Ion Torrent Next Generation Sequencing. For NGS sample preparation, modified primers containing the library primer annealing sites and adapter sequences required for NGS were used to amplify bead-bound ssDNA from the selected rounds. The generated dsDNA was purified using the DNA Clean & Concentrator kit and quantified with the SimpliNANO spectrophotometer. The raw data obtained from NGS for each selection round (in fastq format) were uploaded to the Galaxy webserver (https://usegalaxy.org/) and analyzed as described previously [43]. The data format was converted to fasta, the length of the sequences was constrained to library-length (73–90 bp) and unique overrepresented sequences were identified using the “collapse” tool. To find potentially enterotoxin-binding sequences, the collapsed pools from both CT and LT-ETEC pools were manually compared. The raw data was also analyzed with AptaSuite [44]. Clustal Omega (https://www.ebi.ac.uk/Tools/msa/clustalo/) was used for multiple sequence alignment and identification of sequence families, whereas a sequence motif search was carried out with the MEME tool (https://meme-suite.org/meme/tools/meme). The QGRS Mapper (https://bioinformatics.ramapo.edu/QGRS/index.php) was used to calculate the probabilities of G-quadruplex formation within the selected aptamer sequences.

2.6. Structural characterization of the aptamer candidates with Circular Dichroism and UV thermal melting studies

Aptamer candidates among the top 100 most abundant sequences were chosen for analysis. Specifically, aptamers were dissolved in selection buffer at 1 μM, heated at 95 °C for 5 min and left to slowly cool to room temperature prior to analysis. The Circular Dichroism (CD) spectra were acquired on a Chirascan CD spectrometer (Applied Photophysics, UK) using a 1 cm path length quartz microcuvette in the range of 220–340 nm (1 nm step, adaptive sampling mode). Three spectra were acquired per sample after auto-subtraction of the blank (selection buffer), and the Pro-Data Chirascan software was used for smoothing and averaging the spectra. For UV thermal melting studies, a VARIAN Cary 100 Bio spectrophotometer (Varian Iberica, Spain) equipped with a temperature control accessory was used. The absorbance of the aptamer solutions was recorded at 260 nm over the range of 20–90 °C with heating/cooling rates of 2 °C/min using a 1 cm path length quartz microcuvette. The melting temperature (T_m) for each aptamer was determined from the peak maximum of the first derivative of the absorbance spectra (dA/dT) calculated with GraphPad Prism software. An unrelated aptamer (5′-AGCTCCAGAA GATAAATTAC AGGGAACGTG TTGGTTGCGG TTCTTCCGAT CTGCTGTGTT CTCTATCTGT GCCATGCAAC TAGGATACTA TGACCCCGG-3′) was used as a control.

2.7. Characterization of aptamer candidate binding affinity

The Apta-PCR Affinity Assay (APAA) was used to evaluate the binding affinity of one of the most abundant sequence found in the enriched pools of both enterotoxins (sequence Seq.2) as described previously [45]. Initially, CT and LT-ETEC were immobilized on epoxy-activated magnetic beads as follows: 100 μL of Dynabeads M-270 Epoxy magnetic beads (suspension of 30 mg/mL) were washed with 3 × 100 μL of 0.1 M sodium phosphate pH 7 and then resuspended with 60 μL of 1 mg/mL CT or LT-ETEC in PBS (or only PBS for control-beads) and 60 μL of 3 M ammonium sulphate. The mixtures were incubated overnight at 22 °C under rotation, followed by washing with 500 μL of 0.1 M sodium phosphate pH 7. The beads were blocked with 1 M Tris pH 8.8 for 2 h at 22 °C under rotation, followed by washing (3 × 200 μL of PBST) and resuspension with 100 μL of PBS. The immobilization of the enterotoxins on the beads was confirmed by bead-ELISA as described earlier. Two microliters of each bead type (CT-beads or LT-ETEC-beads) were then incubated with 50 μL of 10 μM–16 nM (serial 1/5 dilutions) of the aptamer candidate in selection buffer for 30 min at 22 °C under rotation. After washing three times with 100 μL of PBST, the beads were resuspended with 20 μL of selection buffer and bound ssDNA was detected after PCR amplification (13 cycles) and agarose gel electrophoresis as discussed earlier. The intensities of the bands for each aptamer concentration were estimated with the ImageJ software (gel analysis option) and were plotted with GraphPad Prism. The data was fitted to the model "Specific binding with Hill Slope" for the calculation of the affinity dissociation constants. Triplicate measurements were performed.

3. Results and discussion

3.1. Selection

To identify aptamers binding to the AB_5 enterotoxins of the CT family (CT and LT-ETEC), the proteins were tethered to magnetic beads thus facilitating the separation of target-bound from unbound sequences during the selection process and immobilization on the beads was verified with a bead-ELISA (SI, Fig. S1). Control magnetic beads, whose amine groups were blocked with sulfo–NHS–acetate, were used for the negative selection to eliminate sequences interacting non-specifically with the surface of the beads. The ssDNA library used for the selection contained a random region of 40 nt flanked by the primer annealing sites of 18 nt each. The library, as well as all the sub-pools prepared before each selection round, were diluted in selection buffer (PBS with 1.5 mM $MgCl_2$) and annealed (heated at 95 °C followed by slow cooling to room temperature) to allow for all the sequences to fold properly.

For the first round, the starting ssDNA library was incubated with the CT-beads for 1 h as a pre-enrichment step, considering the low abundance of each sequence within the random unselected library. For all following rounds, the incubation of the ssDNA pools with the beads was performed for 30 min. Single stranded DNA bound to the CT-beads was then amplified and a sub-pool was prepared for the next round. Negative SELEX was incorporated in round 2, by incubating first the ssDNA sub-pool prepared from the first round with the control-beads. The unbound fraction was then transferred to a tube with CT-beads and a positive selection round was performed. This strategy was followed until round 9, after which the LT-ETEC-beads were incorporated in a step resembling counter SELEX. As commented earlier, CT and LT-ETEC share very high structural and sequence similarity (SI, Fig. S2 and Fig. S3). Whilst we have previously shown that distinct aptamers binding to structurally similar targets can be identified from one single selection when using counter-SELEX-like steps for each different target in combination with NGS [43], it is still likely that selected aptamers can be cross-reacting with both toxins. In this work, two consecutive incubations steps of the ssDNA sub-pools with the two enterotoxins were performed aiming at the enrichment of sequences binding only one or both toxins. Different sequences would allow the differentiation of infections caused by *V. cholerae* and ETEC, while a common sequence could be used for the simultaneous detection of diarrhea-causing enteropathogenic bacteria typically found in water bodies in low- and middle-income countries. During selection round 10, the ssDNA sub-pool was first incubated with the control-beads (negative SELEX), the unbound fraction was then incubated with the LT-ETEC-beads (target 2) and finally with the CT-beads (target 1). The same process was followed until round 20 at which point the selection was concluded. Pilot PCR, i.e. the amplification of a sample using different number of cycles, was performed at the end of each selection round to evaluate the progress and also to determine the number of cycles required for optimal amplification of target-bound ssDNA and preparation of the sub-pool for following rounds.

The evolution of the selection was monitored using pilot PCR and Apta-PCR Affinity Assay (APAA). As shown in Fig. 1A, the amount of ssDNA bound on the CT-beads increased until round 10, after which no further enrichment was observed. Because of the variation of the amount of ssDNA used in each selection round, a second assay was designed to further investigate the progress of the selection with regards to sequences binding to CT which was the final incubation step in each round. For the APAA, ssDNA bound on CT-beads from several selection rounds was prepared and equal concentrations were incubated in parallel with CT-beads. Bound ssDNA was then detected by PCR and the amplicons visualized using agarose gel electrophoresis. The intensity of the bands corresponding to the PCR amplicons for each round was estimated with the ImageJ software as a measure of the amount of bead-bound ssDNA. As the selection progressed, the oligonucleotide sub-pools were enriched in CT-binding sequences up to round 10 and no significant difference was observed after that (Fig. 1B).

3.2. NGS data analysis and identification of aptamer candidates

Oligonucleotides pools from the last selection round bound on both types of enterotoxin beads (R20-CT and R20-LT-ETEC), as well as CT-beads from an early stage of the selection (round 6) were sequenced with NGS to identify CT and LT-ETEC aptamer candidates. The analysis performed using the Galaxy webserver involved filtering of the sequences with length similar to the starting library and identification of unique sequences by data collapsing. PCR and sequencing artifacts were minimal since more than 97% of each dataset contained sequences of the correct size. As can be seen in Table 2, there was enrichment in enterotoxin-binding sequences since the fraction of unique sequences decreased from 98.9% in round 6 (CT-beads) to 34.2% (CT-beads) and 34.9% (LT-ETEC-beads) in the final round. The raw data were also analyzed with AptaSuite, a dedicated software for the analysis of NGS data from SELEX experiments for the identification of aptamer candidates [35]. The overall enrichment in the pools sequenced was evident by the decrease of the unique fraction and increase of the enriched species (SI, Fig. S4).

Looking at the general statistics in Table 2, it can also be observed that the enrichment in enterotoxin-binding sequences was accompanied by an overall increase in the % GC content of the selected oligonucleotide sub-pools. Indeed, the starting random library used for SELEX had a 52% GC content (50% in the 40 nt long random region), confirming the absence of any bias in library construction. The highly diverse pool from round 6 contained 49% GC, whereas the enriched pools from the final selection round (> 65% enrichment) contained 58% GC. Analysis of the NGS data with AptaSuite revealed that this increase in overall GC content stemmed specifically from the increase in guanine residues (G) within the first 20 bases of the random region of the library (SI, Fig. S5). Evidently, there was a tendency of G-rich sequences binding to CT and LT-ETEC enterotoxins.

On the individual sequence level, the top 100 most abundant unique sequences from each round, constituting 3.2–54.8% of the total library-length sequences, were further analyzed (Fig. 2). Sequences with fewer

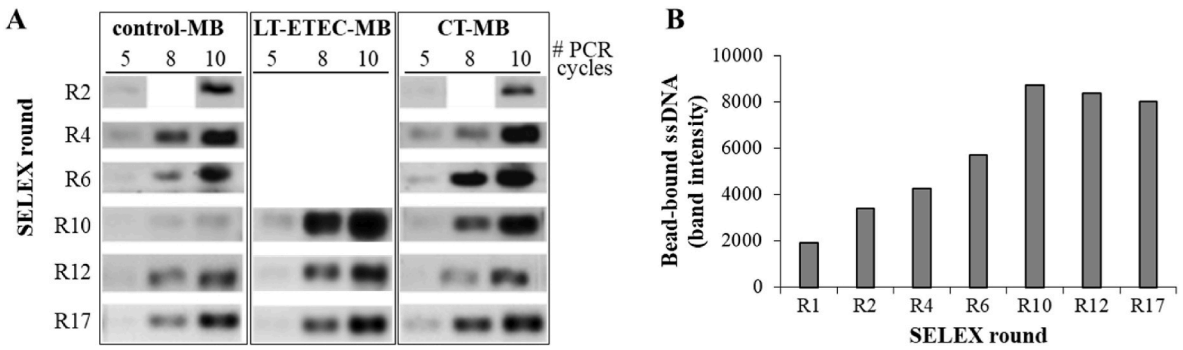

Fig. 1. Evolution of the selection. (A) Pilot PCR performed during the selection for the amplification of bead-bound ssDNA (after 5, 8 or 10 PCR cycles) and analysis by agarose gel electrophoresis. (B) Enrichment of the ssDNA pools from each selection round in CT-binding sequences studied by APAA. After completion of the selection, equal concentration of ssDNA prepared from the CT-beads from each round was incubated with CT-beads, amplified by PCR (10 cycles) and analyzed by agarose gel electrophoresis. The intensities of the bands were estimated with the ImageJ software.

Table 2
Properties of the sequences encountered in the pools sequenced by Ion Torrent NGS.

Selection round	% GC	Filtered	Unique (%)	% Enrichment	Top 100 (%)	Top 10 (%)
R6-CT	49	4621	4571 (98.9)	1.1	150 (3.2)	20 (0.4)
R20-CT	58	5642	1931 (34.2)	65.8	3089 (54.8)	1271 (22.5)
R20-LT-ETEC	58	5080	1773 (34.9)	65.1	2774 (54.6)	1161 (22.9)

than 7 copies were not included in the analysis. The insignificant enrichment of the pool from the initial stage of the selection (R6-CT) was evident by the multitude of low-frequency unique sequences (0.7–1.3%). On the other hand, higher frequencies were observed at the end of the selection (0.2–7.3% in R20-CT and 0.3–8.5% in R20-LT-ETEC). Clustal Omega was used for the alignment of these sequences in search of sequence families, but none were found. On the other hand, when a sequence motif search was conducted with the MEME tool, a dominant G-rich motif was identified in all of the top 100 sequences from the last selection round (Fig. 2). This is consistent with the high % G within the random region of the sequences from the enriched pools as discussed earlier. It was thus hypothesized that this is a CT/LT-ETEC enterotoxin-binding sequence motif since it was found in both pools. Because of the prevalence of this G-rich motif, the possibility of G-quadruplex formation was explored using the QGRS Mapper. This tool was used to calculate the G-scores which represent the likelihood to form stable G-quadruplexes. After analyzing the top 10 most abundant sequences from each enriched pool, high G-score values were calculated for all sequences, in the range of 20–42 (SI, Table S1). Overall, these results suggest that aptamers binding to AB_5 enterotoxins of the CT family which includes CT and LT-ETEC tend to fold into G-quadruplexes. Interestingly, the only other selection reported in the literature for CT aptamers, which targeted only the B subunit, also reported some G-rich sequences and three of them were confirmed to form G-quadruplexes [46].

Alignment of the 10 sequences with the highest frequency from the two enterotoxin-binding pools further highlighted the similarities between them (Fig. 3). In fact, there were several conserved sequences in both CT and LT-ETEC pools (boxed sequences). And all 20 sequences contained the dominant G-rich sequence motif. Overall, the NGS data suggest that the selection resulted in the enrichment of common enterotoxin binders, while no sequence specific to only one of the enterotoxins was encountered.

3.3. *Evaluation of the structural conformation of aptamer candidates*

In silico analysis of enriched sequences suggested that they could potentially contain G-quadruplex sub-structures. To confirm this hypothesis experimentally, selected aptamer candidates were characterized with Circular Dichroism (CD) and UV thermal melting studies. CD spectroscopy allows the differentiation of DNA molecules containing stem-loop structures from G-quadruplexes: peak maximum at 275 nm and minimum at 245 nm are characteristic of stem-loop structures, whereas parallel and anti-parallel G-quadruplexes show dominant peak maximums at around 265 nm and 295 nm, respectively [47]. In this work, selected aptamer sequences were analyzed, along with an

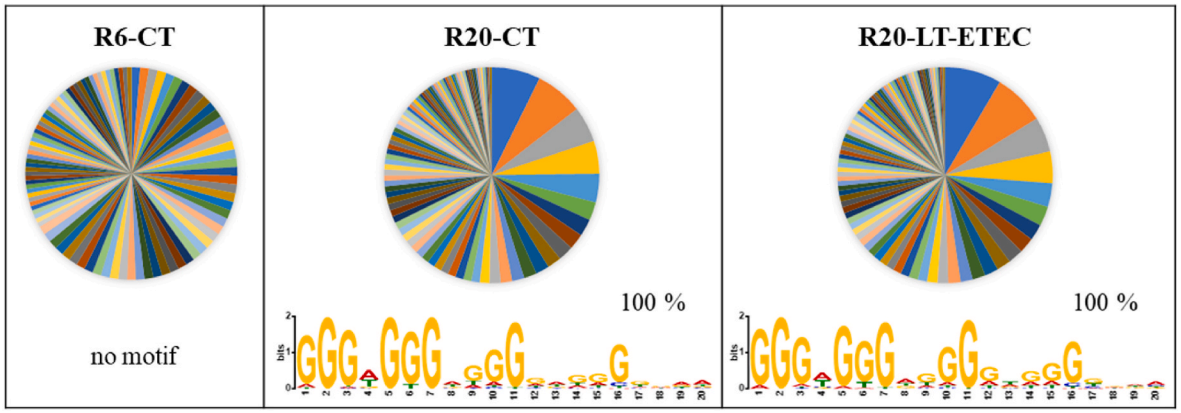

Fig. 2. Composition of the top 100 most abundant unique sequences in the pools sequenced. The sequence logos of the motifs found within these sequences using MEME suite and its prevalence among them is also shown.

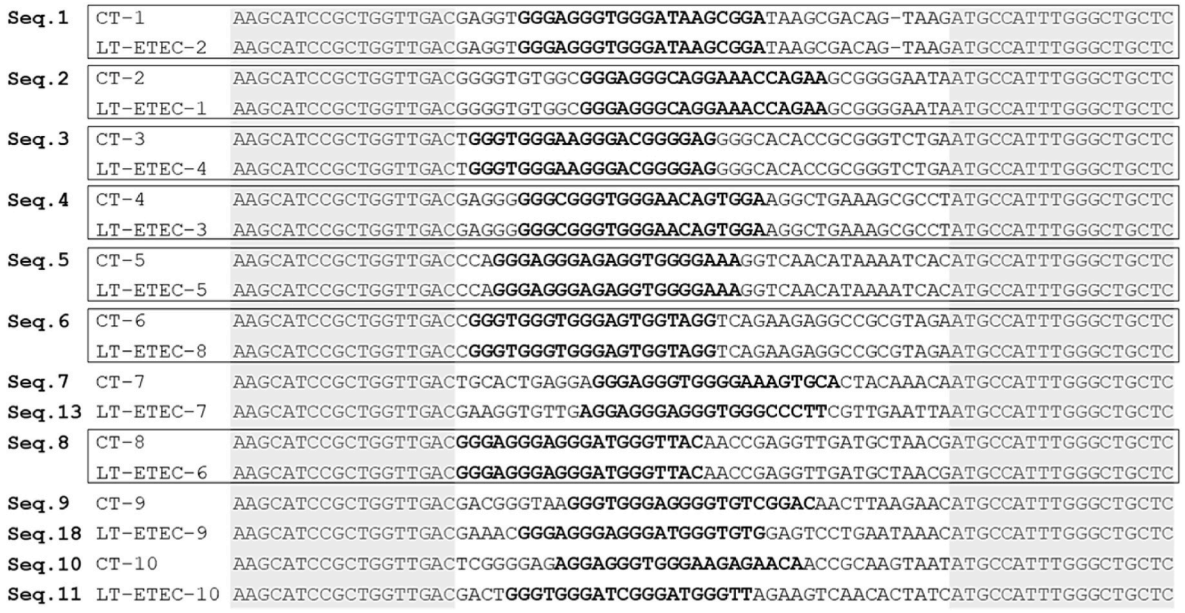

Fig. 3. Alignment of the 10 most abundant sequences from each enriched pool of the final selection round. The primer annealing sites are shaded in grey, identical sequences are boxed and the common G-rich motif is in bold. Sequence IDs were based on the abundance in the CT pool.

unrelated aptamer previously shown to fold in stem-loop conformation [48]. As can be seen in Fig. 4, the control aptamer showed a CD spectrum consistent with stem-loops, with a CDmax at 278 nm. Similar spectral profile was observed for Seq.87 and partially for Seq.41. On the other hand, broad CDmax peaks were observed for Seq.1, Seq.2 and Seq.4 with a clear bathochromic shift to ≤272 nm, indicative of parallel G-quadruplex sub-structures forming within the aptamer sequences. Considering that only parts and not the entire full-length aptamer sequences are expected to participate in the formation of the G-quadruplex structures, a partial and not a complete shift of the CDmax to 265 nm is reasonable. UV thermal melting curves were also acquired to evaluate the stability of the aptamer candidates (SI, Fig. S6A). The melting temperatures (Tm) of Seq.1, Seq.2 and Seq.4 were calculated at > 54 °C, whereas for Seq.41 it was 52 °C and for Seq. 87 and the control aptamer ≤ 39 °C (Table 3 and SI, Fig. S6B). These results suggest higher structural stability of the aptamers Seq.1, Seq.2 and Seq.4, consistent with G-quadruplex structures [49], compared to Seq.87 and the control aptamer which form stem-loops according to the CD studies. For Seq.41, the results from both CD and UV thermal melting studies are not conclusive, potentially suggesting the adoption of mixed conformations

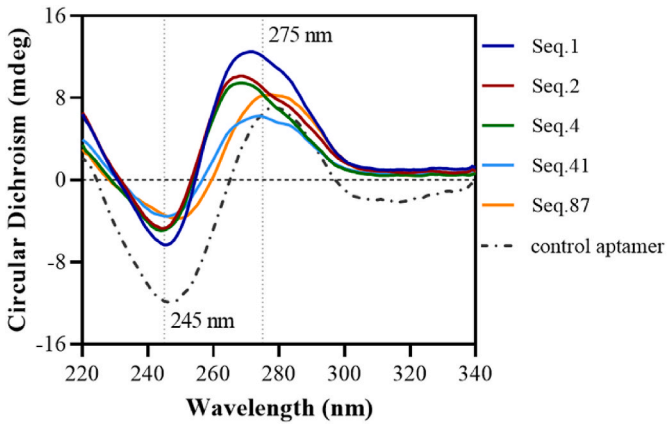

Fig. 4. Circular Dichroism (CD) spectra of selected aptamer candidates. The positions for the CD_{max} (275 nm) and CD_{min} (245 nm) characteristic of aptamers with stem-loop structures are shown.

Table 3
Properties of selected aptamer candidates. The G-score was predicted with the QGRS Mapper, the CDmax from the CD spectra (Fig. 4) and the melting temperature (Tm) from the first derivative of the melting curves (Figs. S6, SI).

Aptamer	% G	G-score	CD_{max} (nm)	Tm (°C)
Seq.1	39	21	272	54
Seq.2	41	21	269	60
Seq.4	41	41	269	54
Seq.41	37	41	274	52
Seq.87	38	20	278	39
control	25	0	278	36

of the particular sequence. Overall, these studies confirm the formation of G-quadruplex sub-structures among the aptamer candidates, especially in Seq.2, which was chosen as a promising aptamer candidate for the detection of both enterotoxins.

3.4. Binding properties of the enterotoxin aptamer candidate

To determine the binding affinity of the chosen aptamer candidate Seq.2, one of the most abundant G-quadruplex sequences from the last selection round, a magnetic bead assay was designed employing conditions similar to those used during the selection. CT and LT-ETEC were immobilized on magnetic beads but via their amine groups rather the carboxylic ones which were targeted for the preparation of the beads used for the selection to eliminate any possible non-specific interactions with the surface of the beads alone. A range of aptamer concentrations (16 nM–10 μM) were incubated in parallel with a constant amount of CT-beads or LT-ETEC-beads and bound aptamer was detected after PCR amplification and agarose gel electrophoresis. The affinity dissociation constants (K_D) of the aptamer for the two enterotoxins were identical, 358 nM for CT and 343 nM for LT-ETEC (Fig. 5). This result confirmed that the Seq.2 sequence is an aptamer binding to AB_5 enterotoxins of the CT family, reinforcing the notion that G-quadruplexes tend to bind AB_5 enterotoxins. Therefore, it could be potentially used for the detection of diarrhea-causing toxins produced by both *V. cholerae* and enterotoxigenic *E. coli* in environmental or clinical isolates. Stool analysis offers the possibility of direct enterotoxin detection [50,51], thus eliminating the time-consuming step of culturing suspicious samples to induce

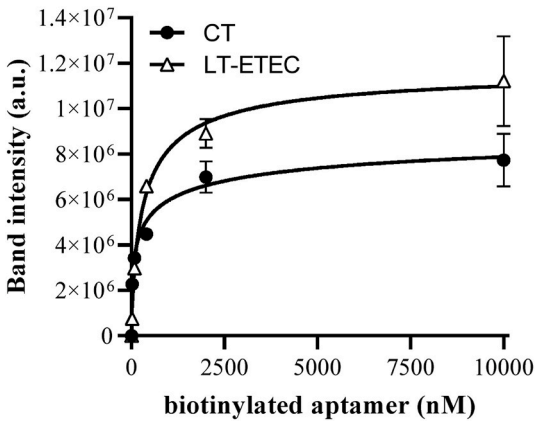

Fig. 5. Binding affinity saturation curves of Seq.2 aptamer with CT and LT-ETEC enterotoxins immobilized on magnetic beads.

enterotoxin secretion. Considering the low concentrations of enterotoxins in stool, the aptamer could be immobilized on magnetic beads for both capture and pre-concentration of enterotoxins in stool samples after simple processing steps as reported previously [52]. Optical, fluorescent, or electrochemical platforms could be designed for enterotoxin detection, while final confirmation of the enterobacteria causing the infection could be provided by DNA amplification techniques. An antibody recognizing both enterotoxins has also been reported in the literature for the co-detection of the two toxins [53], while the Oxoid™ VET-RPLA Toxin Detection Kit from Thermo Scientific is an antibody-based kit commercially available also for the co-detection of the two enterotoxins.

As commented earlier, there are only two reports in the literature on selections for aptamers against AB_5 enterotoxins of the CT family. The first one targeted the whole CT complex which was immobilized on magnetic beads. Even though sequencing was not carried out to identify definite ssDNA sequences, direct binding of labeled CT to the enriched ssDNA pool from the final selection round immobilized on magnetic beads, which was considered as a "polyclonal" aptamer, allowed the detection of < 40 ng of CT [41]. The second selection was reported more than 15 years later and it targeted the B subunit of the toxin alone, which was also immobilized on magnetic beads [42]. Several aptamer candidates with high binding affinity were identified (K_Ds of 23–55 nM), with more than 50% of those containing a G-rich sequence motif, while 3 out of the 8 sequences were confirmed to form G-quadruplexes. One of the non-G-quadruplexes was used to develop a hybrid aptamer-antibody sandwich assay on magnetic beads, while several lateral flow assay designs exploiting sandwich formats of the same aptamer with the antibody or the GM1 receptor were demonstrated in their subsequent work [36]. In all three studies, the authors emphasized the problems encountered in their search for aptamer pairs to be used in a sandwich assay, while Bruno and Kiel [31] concluded that this could potentially suggest a lack of different aptamer binding sites in some protein toxins, especially when they are immobilized. Our work reinforces this hypothesis because of the unequivocal enrichment of a single G-rich sequence motif by the end of the selection. Overall, it appears that AB_5 enterotoxins of the CT family (including CT and LT-ETEC) or their B subunits alone (typically found as a B_5 homopentamers), provide limited binding sites for aptamers on their surface, preventing the simultaneous binding of different aptamers. Moreover, there is a certain predisposition of G-rich, potentially G-quadruplex-forming sequences to bind enterotoxins of this family. This might be attributed to the oligonucleotide/oligosaccharide-binding fold (OB-fold) of the B subunit of both CT [54] and LT-ETEC, which has been demonstrated to be one of the structural properties and protein folds promoting binding of G-quadruplexes [55]. This could explain the convergence of the selection to identical sequences against both enterotoxins presumably against a single dominant binding site considering the extremely high structural and sequence similarities between them. Moreover, the Seq.2 aptamer, whose binding to both CT and LT-ETEC was demonstrated, was confirmed to fold into a G-quadruplex. It should be noted that their high thermodynamic and chemical stability together with improved electrostatic interactions render G-quadruplexes advantageous to unstructured sequences for the development of aptasensors [56].

4. Conclusions

This work sought to generate ssDNA aptamers against AB_5 enterotoxins of the cholera toxin family as specific biorecognition molecules for the detection of infections caused by both *V. cholerae* and enterotoxigenic *E. coli*. These could be used as tools for the development of tests compatible with low resource settings for preventing and controlling diarrheal diseases caused by these two bacteria frequently encountered in low-to middle-income countries. Using the CT and LT-ETEC proteins immobilized on magnetic beads and a random ssDNA library of 76 nt, SELEX was performed for 20 rounds implemented by negative (control beads) to improve specificity. Enriched pools were sequenced by NGS and in-depth bioinformatic analysis revealed selective enrichment in sequences with high % GC content. Furthermore, a dominant G-rich sequence motif was discovered in the sequences of the final selection round which were conserved in both the CT and LT-ETEC pools. CD spectroscopy and UV thermal melting curve analysis confirmed G-quadruplex folding in highly abundant sequences. Binding studies showed that one of the most abundant sequences encountered in both enriched pools folding into a G-quadruplex recognized equally the two enterotoxins (K_D values of 343 and 358 nM), demonstrating its suitability for co-detection of the two toxins and indirectly of the enterobacteria producing them. A dominant binding site on the surface of the two proteins could be presumably responsible for the convergence of the selection to common G-rich binding sequences. The work shown herein is in accordance with the only other previous report on the selection of aptamers against enterotoxins of the cholera toxin family, in which G-rich and G-quadruplex folding sequences were selected presumably against a common binding site, while sandwich formats with only non-aptamer biorecognition elements were possible for detection. Further work will focus on the comprehensive characterization of the selected aptamer and its application in bioanalytical assays for the environmental surveillance of epidemic cholera and milder diarrheal disease caused by enterotoxigenic *E. coli*.

CRediT authorship contribution statement

Nerissa A. Molejon: Experimental work. **Catherine M. Lapada:** Experimental work. **Vasso Skouridou:** Experimental work, Drafting and revision of manuscript. **Analiza P. Rollon:** Supervision, Experimental Planning, revision of manuscript. **Mohammed El-Shahawi:** Supervision, Experimental Planning, revision of manuscript. **Abdulaziz Bashammakh:** Supervision, Experimental Planning, revision of manuscript. **Ciara K. O'Sullivan:** Financing, Supervision, Experimental Planning, drafting and revision of manuscript.

Declaration of competing interest

The authors declare that they have no known competing financial interests or personal relationships that could have appeared to influence the work reported in this paper.

Data availability

Data will be made available on request.

Acknowledgements

This research was funded by the University of the Philippines Systems Office of International Linkages through the COOPERATE program, Engineering Research and Development for Technology of the Department of Science and Technology, Republic of the Philippines, and by the Interfibio Research Group at Universitat Rovira i Virgili, Tarragona, Spain. The following reagent was obtained through BEI Resources, NIAID, NIH: Enterotoxigenic *Escherichia coli* Double Mutant Heat-Labile Toxoid (dmLT), Adjuvant-Active, Recombinant from *Escherichia coli*, NR-51683.

Appendix A. Supplementary data

Supplementary data to this chapter can be found online at https://doi.org/10.1016/j.ab.2023.115118.

References

[1] S.M. Fletcher, M.L. McLaws, J.T. Ellis, Prevalence of gastrointestinal pathogens in developed and developing countries: systematic review and meta-analysis, J. Public Health Res. 2 (2013) 42–53, https://doi.org/10.4081/jphr.2013.e9.

[2] C.M.A. P Franz, H.M.W. den Besten, C. Bohnlein, M. Gareis, M.H. Zwietering, V. Fusco, Microbial food safety in the 21st century: emerging challenges and foodborne pathogenic bacteria, Trends Food Sci. Technol. 81 (2018) 155–158, https://doi.org/10.1016/j.tifs.2018.09.019.

[3] M.D. Kirk, S.M. Pires, R.E. Black, M. Caipo, J.A. Crump, B. Devleesschauwer, et al., World Health Organization estimates of the global and regional disease burden of 22 foodborne bacterial, protozoal, and viral diseases, 2010: a data synthesis, PLoS Med. 12 (12) (2015), e1001921, https://doi.org/10.1371/journal.pmed.1001921.

[4] J. Sell, B. Dolan, Common gastrointestinal infections, Prim. Care, Clin. Office Pract. 45 (2018) 519–532, https://doi.org/10.1016/j.pop.2018.05.008.

[5] J.E. Heggelund, V.A. Bjornestad, U. Krengel, Vibrio cholerae and Escherichia coli heat-labile enterotoxins and beyond, in: J. Alouf, D. Ladant, M.R. Popoff (Eds.), The Comprehensive Sourcebook of Bacterial Protein Toxins, fourth ed., Elsevier Ltd, 2015, pp. 195–229, https://doi.org/10.1016/B978-0-12-800188-2.00007-0.

[6] J.D. Forbes, Clinically important toxins in bacterial infection: utility of laboratory detection, Clin. Microbiol. Newsl. 42 (2020) 163–170, https://doi.org/10.1016/j.clinmicnews.2020.09.003.

[7] R.R. Colwell, Global climate and infectious disease: the cholera paradigm, Science 274 (1996) 2025–2031, https://doi.org/10.1126/science.274.5295.2025.

[8] S. Kanungo, A.S. Azman, T. Ramamurthy, J. Deen, S. Dutta, Cholera, Lancet 399 (2022) 1429–1440, https://doi.org/10.1016/S0140-6736(22)00330-0.

[9] World Health Organization, Cholera. https://www.who.int/news-room/fact-sheets/detail/cholera#:~:text=of%20social%20development.,Symptoms,kill%20within%20hours%20if%20untreated. (Accessed 19 May 2022).

[10] M. Ali, A.R. Nelson, A.L. Lopez, D.A. Sack, Updated global burden of cholera in endemic countries, PLoS Neglected Trop. Dis. 9 (2015), e0003832, https://doi.org/10.1371/journal.pntd.0003832.

[11] L. Gonzalez-Siles, A. Sjoling, The different ecological niches of enterotoxigenic Escherichia coli, Environ. Microbiol. 18 (2016) 741–751, https://doi.org/10.1111/1462-2920.13106.

[12] Q. Duan, P. Xia, R. Nandre, W. Zhang, G. Zhu, Review of newly identified functions associated with the heat-labile toxin of enterotoxigenic Escherichia coli, Front. Cell. Infect. Microbiol. 9 (2019) 292, https://doi.org/10.3389/fcimb.2019.00292.

[13] E.N. Biernbaum, I.T. Kudva, AB5 enteroxotin-mediated pathogenesis: perspectives gleaned from Shiga toxins, Toxins 14 (2022) 62, https://doi.org/10.3390/toxins14010062.

[14] R.G. Zhang, D.L. Scott, M.L. Westbrook, S. Nance, B.D. Spangler, G.G. Shipley, E. M. Westbrook, The three-dimensional crystal structure of cholera toxin, J. Mol. Biol. 251 (1995) 563–573, https://doi.org/10.1006/jmbi.1995.0456.

[15] J.B. Kaper, J.G. Morris Jr., M.M. Levine, Cholera, Clin. Microbiol. Rev. 8 (1995) 48–86, https://doi.org/10.1128/CMR.8.1.48.

[16] F. Cecchini, L. Fajs, S. Cosnier, R.S. Marks, Vibrio cholerae detection: traditional assays, novel diagnostic techniques and biosensors, TrAC - Trends Anal. Chem. 79 (2016) 199–209, https://doi.org/10.1016/j.trac.2016.01.017.

[17] World Health Organization, WHO Preferred Product Characteristics for Vaccines against Enterotoxigenic Escherichia coli (ETEC), 2021. https://www.who.int/publications/i/item/who-preferred-product-characteristics-for-vaccines-against-enterotoxigenic-escherichia-coli. (Accessed 13 September 2022).

[18] D.W. Pimbley, P.D. Patel, A review of analytical methods for the detection of bacterial toxins, J. Appl. Microbiol. Symp. Suppl. 84 (1988), https://doi.org/10.1046/j.1365-2672.1998.0840s198s.x, 98S–109S.

[19] US Centers for Disease Control and Prevention, Laboratory testing for cholera. https://www.cdc.gov/cholera/pdf/laboratory-methods-for-the-diagnosis-of-vibrio-cholerae-chapter-7.pdf. (Accessed 19 May 2022).

[20] A.J. Gubala, Multiplex real-time PCR detection of Vibrio cholerae, J. Microbiol. Methods 65 (2006) 278–293, https://doi.org/10.1016/j.mimet.2005.07.017.

[21] J.A. Grembi, K. Mayer-Blackwell, S.P. Luby, A.M. Spormann, High-throughput multiparallel enteropathogen detection via nano-liter qPCR, Front. Cell. Infect. Microbiol. 10 (2020) 351, https://doi.org/10.3389/fcimb.2020.00351.

[22] C. Rodas, V. Iniguez, F. Qadri, G. Wiklund, A.M. Svennerholm, A. Sjoling, Development of multiplex PCR assays for detection of enterotoxigenic Escherichia coli colonization factors and toxins, J. Clin. Microbiol. 47 (2009) 1218–1220, https://doi.org/10.1128/JCM.00316-09.

[23] W. Yamazaki, K. Seto, M. Taguchi, M. Ishibashi, K. Inoue, Sensitive and rapid detection of cholera toxin-producing Vibrio cholerae using a loop-mediated isothermal amplification, BMC Microbiol. 8 (2008) 94, https://doi.org/10.1186/1471-2180-8-94.

[24] M. Xu, H. Fu, D. Chen, Z. Shao, J. Zhu, W.Q. Alali, L. Chen, Simple visualized detection method of virulence-associated genes of Vibrio cholerae by loop-mediated isothermal amplification, Front. Microbiol. 10 (2019), https://doi.org/10.3389/fmicb.2019.02899.

[25] A. Yano, R. Ishimaru, R. Hujikata, Rapid and sensitive detection of heat-labile I and heat-stable I enterotoxin genes of enterotoxigenic Escherichia coli by loop-mediated isothermal amplification, J. Microbiol. Methods 68 (2007) 414–420, https://doi.org/10.1016/j.mimet.2006.09.024.

[26] S. Seherler, A. Bozdogan, T.A. Ozal Ildeniz, F.N. Kok, I. Anac Sakir, Detection of cholera toxin with surface plasmon field-enhanced fluorescent spectroscopy, Biotechnol. Appl. Biochem. (2021) 1–10, https://doi.org/10.1002/bab.2227.

[27] C.Y. Yu, G.Y. Ang, K.G. Chan, K.K. Banga Singh, Y.Y. Chan, Enzymatic electrochemical detection of epidemic-causing Vibrio cholerae with a disposable oligonucleotide-modified screen-printed bisensor coupled to a dry-reagent-based nucleic acid amplification assay, Biosens. Bioelectron. 70 (2015) 282–288, https://doi.org/10.1016/j.bios.2015.03.048.

[28] T. Peng, Q. Cheng, R.C. Stevens, Amperometric detection of Escherichia coli heat-labile enterotoxin by redox diacetylenic vesciles on a sol–gel thin-film electrode, Anal. Chem. 72 (2000) 1611–1617, https://doi.org/10.1021/ac990406y.

[29] M.M. Habibi, S.A. Mirhosseini, S. Sajjadi, A.H. Keihan, A novel label-free electrochemical immunesensor for ultrasensitive detection of LT toxin using prussian blue@gold nanoparticles composite as a signal amplification, Bioelectrochemistry 142 (2021), 107887, https://doi.org/10.1016/j.bioelechem.2021.107887.

[30] T. Ramamurthy, B. Das, S. Chakraborty, A.K. Mukhopadhyay, D.A. Sack, Diagnostic techniques for rapid detection of Vibrio cholerae O1/O139, Vaccine 38 (Suppl 1) (2020) A73–A82, https://doi.org/10.1016/j.vaccine.2019.07.099.

[31] C. Henrique, B.A. Caetano, T. Mitsunari, L.F. dos Santos, R.M.F. Piazza, L.B. Rocha, Large-scale evaluation of a rapid diagnostic test for diarrhea caused by enterotoxigenic Escherichia coli targeting the heat-labile toxin, J. Microbiol. Methods 144 (2018) 125–127, https://doi.org/10.1016/j.mimet.2017.11.020.

[32] World Health Organization, Global Task Force on cholera control surveillance laboratory working group, The use of cholera rapid diagnostic tests, https://www.gtfcc.org/wp-content/uploads/2019/10/gtfcc-interim-use-of-cholera-rapid-diagnostic-tests.pdf. (Accessed 19 May 2022).

[33] B.A. Muzembo, K. Kitahara, A. Debnath, K. Okamoto, S.I. Miyoshi, Accuracy of cholera rapid diagnostic tests: a systematic review and meta-analysis, Clin. Microbiol. Infect. 28 (2022) 155–162, https://doi.org/10.1016/j.cmi.2021.08.027.

[34] C. Tuerk, L. Gold, Systematic evolution of ligands by exponential enrichment: RNA ligands to bacteriophage T4 DNA polymerase, Science 249 (1990) 505–510, https://doi.org/10.1126/science.2200121.

[35] A.D. Ellington, J.W. Szostak, In vitro selection of RNA molecules that bind specific ligands, Nature 346 (1990) 818–822, https://doi.org/10.1038/346818a0.

[36] L.S. Liu, F. Wang, Y. Ge, P.K. Lo, Recent developments in aptasensors for diagnostic applications, ACS Appl. Mater. Interfaces 13 (2021) 9329–9358, https://doi.org/10.1021/acsami.0c14788.

[37] L.A. Stanciu, Q. Wei, A.K. Barui, N. Mohammad, Recent advances in aptamer-based biosensors for global health applications, Annu. Rev. Biomed. Eng. 23 (2021) 433–459, https://doi.org/10.1146/annurev-bioeng-082020-035644.

[38] M. Citartan, T.H. Tang, Recent developments of aptasensors expedient for point-of-care (POC) diagnostics, Talanta 199 (2019) 556–566, https://doi.org/10.1016/j.talanta.2019.02.066.

[39] J. Teng, F. Yuan, Y. Ye, L. Zheng, L. Yao, F. Xue, W. Chen, B. Li, Aptamer-based technologies in foodborne pathogen detection, Front. Microbiol. 7 (2016) 1426, https://doi.org/10.3389/fmicb.2016.01426.

[40] N. Alizadeh, M.Y. Memar, B. Mehramuz, S.S. Abibiglou, F. Hemmati, H. Samati Kafil, Current advances in aptamer-assisted technologies for detecting bacterial and fungal toxins, J. Appl. Microbiol. 124 (2017) 644–651, https://doi.org/10.1111/jam.13650.

[41] J.G. Bruno, J.L. Kiel, Use of magnetic beads in selection and detection of biotoxin aptamers by electrochemiluminescence and enzymatic methods, Biotechniques 21 (2002) 178–180, https://doi.org/10.2144/02321dd04.

[42] E. Frohnmeyer, F. Frisch, S. Falke, C. Betzel, M. Fischer, Highly affine and selective aptamers against cholera toxin as capture elements in magnetic bead-based sandwich ELAA, J. Biotechnol. 269 (2018) 35–42, https://doi.org/10.1016/j.jbiotec.2018.01.012.

[43] M. Jauset-Rubio, M.L. Botero, V. Skouridou, G.B. Aktas, M. Svobodova, A. S. Bashammakh, A.O. Alyoubi, C.K. O'Sullivan, One-pot SELEX: identification of specific aptamers against diverse steroid targets in one selection, ACS Omega 4 (2019) 20188–20196, https://doi.org/10.1021/acsomega.9b02412.

[44] J. Hoinka, R. Backofen, T.M. Przytycka, AptaSUITE: a full-featured bioinformatics framework for the comprehensive analysis of aptamers from HT-SELEX experiments, Mol. Ther. Nucleic Acids 11 (2018) 515–517, https://doi.org/10.1016/j.omtn.2018.04.006.

[45] X. Shkembi, V. Skouridou, M. Svobodova, S. Leonardo, A.S. Bashammakh, A. O. Alyoubi, M. Campas, C.K. O'Sullivan, Hybrid antibody-aptamer assay for detection of tetrodotoxin in pufferfish, Anal. Chem. 93 (2021) 14810–14819, https://doi.org/10.1021/acs.analchem.1c03671.

[46] E. Frohnmeyer, N. Tuschel, T. Sitz, C. Hermann, G.T. Dahl, F. Schulz, A. J. Baeumner, M. Fischer, Aptamer lateral flow assays for rapid and sensitive detection of cholera toxin, Analyst 144 (2019) 1840–1849, https://doi.org/10.1039/c8an01616j.

[47] J. Kypr, I. Kejnovska, D. Renciuk, M. Vorlickova, Circular dichroism and conformational polymorphism of DNA, Nucleic Acids Res. 37 (2009) 1713–1725, https://doi.org/10.1093/nar/gkp026.

[48] T. Mairal Lerga, M. Jauset-Rubio, V. Skouridou, A.S. Bashammakh, M.S. El-Shahawi, A.O. Alyoubi, C.K. O'Sullivan, High affinity aptamer for the detection of the biogenic amine histamine, Anal. Chem. 91 (2019) 7104–7111, https://doi.org/10.1021/acs.analchem.9b00075.

[49] J.L. Mergny, L. Lacroix, Analysis of thermal melting curves, Oligonucleotides 13 (2003) 515–537, https://doi.org/10.1089/154545703322860825.

[50] T. Ramamurthy, S.K. Bhattacharya, Y. Uesaka, K. Horigome, M. Paul, D. Sen, S. C. Pal, T. Takeda, Y. Takeda, G.B. Nair, Evaluation of the bead enzyme-linked immunosorbent assay for detection of cholera toxin directly from stool specimens, J. Clin. Microbiol. 30 (1992) 1783–1786, https://doi.org/10.1128/jcm.30.7.1783-1786.

[51] M.H. Merson, R.H. Yolken, R.B. Sack, J.L. Froehlich, H.B. Greenberg, I. Huq, R. W. Black, Detection of Escherichia coli enterotoxins in stool, Infect. Immun. 29 (1980) 106–113, https://doi.org/10.1128/iai.29.1.108-113.

[52] N. Bunyakul, C. Promptmas, A.J. Baeumner, Microfluidic biosensor for cholera toxin detection in fecal samples, Anal. Bioanal. Chem. 407 (2015) 727–736, https://doi.org/10.1007/s00216-014-7947-9.

[53] H. Arimitsu, K. Sasaki, T. Tsuji, Immunochromatographic detection of the heat-labile enterotoxin of enterotoxigenic Escherichia coli with cross-detection of cholera toxin, J. Microbiol. Methods 132 (2017) 148–152, https://doi.org/10.1016/j.mimet.2016.12.007.

[54] K. Ginalski, L. Kinch, L. Rychlewski, N.V. Grishin, BOF: a novel family of bacterial OB-fold proteins, FEBS Lett. 567 (2004) 297–301, https://doi.org/10.1016/j.febslet.2004.04.086.

[55] H. Shu, R. Zhang, K. Xiao, J. Yang, X. Sun, G-quadruplex-binding proteins: promising targets for drug design, Biomolecules 12 (2022) 648, https://doi.org/10.3390/biom12050648.

[56] C. Roxo, W. Kotkowiak, A. Pasternak, G-quadruplex-forming aptamers–characteristics, applications, and perspectives, Molecules 24 (2019) 3781, https://doi.org/10.3390/molecules24203781.